INTERNATIONAL JOURNAL FOR NUMERICAL METHODS IN FLUIDS, VOL. 25, 143–149 (1997)

SUBGRID VOLUMETRIC QUADRATURE ACCURACY FOR TRANSIENT COMPRESSIBLE FLOW PREDICTIONS

G. F. NATERER*

Department of Mechanical Engineering, Lakehead University, 955 Oliver Rd, Thunder Bay, Ontario, Canada P7B 5E1

SUMMARY

A finite volume–element formulation of the Navier–Stokes equations for compressible flows is applied to the transient shock tube problem. A second-order spatial quadrature for volumetric integration is studied because of its effects on the shock wave resolution and positioning. Low quadrature order is shown to produce solution anomalies in regions with a transonic character as well as poor predictions of shock wave propagation. The second-order volumetric quadrature includes the proper upstream and downstream solution behaviour and eliminates both the transonic and shock speed errors in the transient shock tube problem. © 1997 by John Wiley & Sons, Ltd.

Int. J. Numer. Meth. Fluids, **25**: 143–149 (1997).

No. of Figures: 2. No. of Tables: 0. No. of References: 11.

KEY WORDS: transient compressible flow; finite element; quadrature

INTRODUCTION

The overall strategy of modern computational methods for compressible flows presents a difficult dilemma. Most numerical methods begin with the differential equations for conservation of mass, momentum and energy and discretize these equations by finite differences,[1,2] elements[3,4] or volumes.[5,6] The schemes will then refine the discrete model to return and approach the original fine-scale equations. However, the original differential equations appear unnecessary in a sense, because the algebraic equations may be derived by an application of conservation principles to discrete control volumes.

The role of subgrid (i.e. subelement or subvolume) approximations inherent in the models presents a question. Should the model incorporate a coarse grid (in relative terms) with high subgrid quadrature accuracy or a fine grid with low subgrid quadrature accuracy? In particular, previous researchers have presented limited treatments of subgrid quadrature effects on compressible flow phenomena, i.e. shock wave propagation.

For example, a 'zero energy mode' problem associated with low-order quadrature may lead to a singular stiffness matrix in finite element analysis. In this problem a non-zero response throughout the element (i.e. non-zero energy flow) except at the quadrature points (i.e. line of symmetry) may lead to a singular stiffness matrix which would preclude a solution.[7]

In compressible flows the continuity equation acts as a transport equation for the gas density. Subgrid quadratures for the transient effects must yield the correct solution behaviour in different

*Correspondence to: G.F. Naterer, Department of Mechanical Engineering, Lakehead University, 955 Oliver Rd, Thunder Bay, Ontario, Canada P7B 5E1

CCC 0271–2091/97/020143–07 $17.50 *Received 30 June 1995*
© 1997 by John Wiley & Sons, Ltd.

flow regimes. For instance, the character of the transport equation must be elliptic in the subsonic regime and hyperbolic in the supersonic regime. Limited treatments of the former transient effects have been presented in the literature, because as grid refinement is effected, the quadrature analysis becomes less critical in the model. However, the quadrature error must remain less than the discretization error in order to ensure the scheme's order accuracy.

In this paper the details of a second-order volumetric quadrature are presented and the effects on solution accuracy are examined. The volumetric quadrature includes both subelement and element node influences to eliminate pressure oscillations in the transonic region and enhance the scheme's shock-capturing capabilities.

2. PROBLEM FORMULATION

The governing equations for viscous compressible fluid flow and heat transfer are the Navier–Stokes equations

$$\frac{\partial \Phi}{\partial t} + \nabla \cdot \vec{F} = S_\phi, \qquad \vec{\Phi} = (\rho, \rho u, \rho v, \rho e), \tag{1}$$

where ρ, u, v and e represent density, Cartesian velocity components and total energy per unit mass respectively. The vectors $\vec{F}$ consists of advective, $\vec{F}^{\mathrm{a}}$, and diffusive, $\vec{F}^{\mathrm{d}}$, components:

$$\vec{F}^{\mathrm{a}} = \begin{pmatrix} \rho u & \rho v \\ \rho u u + p & \rho u v \\ \rho v u & \rho v v + p \\ (\rho e + p)u & (\rho e + p)v \end{pmatrix}, \tag{2}$$

$$\vec{F}^{\mathrm{d}} = \begin{pmatrix} 0 & 0 \\ -\tau_{xx} & -\tau_{xy} \\ -\tau_{yx} & -\tau_{yy} \\ -u\tau_{xx} - v\tau_{xy} + q_x & -u\tau_{xy} - v\tau_{yy} + q_y \end{pmatrix}. \tag{3}$$

The components of the stress tensor and heat flux vector are

$$\tau_{xx} = 2\mu \frac{\partial u}{\partial x} - \frac{2}{3}\mu \left(\frac{\partial u}{\partial x} + \frac{\partial v}{\partial y} \right), \tag{4}$$

$$\tau_{xy} = \mu \left(\frac{\partial u}{\partial y} + \frac{\partial v}{\partial x} \right) = \tau_{yx}, \tag{5}$$

$$\tau_{yy} = 2\mu \frac{\partial v}{\partial y} - \frac{2}{3}\mu \left(\frac{\partial u}{\partial x} + \frac{\partial v}{\partial y} \right), \tag{6}$$

$$q_x = -k \frac{\partial T}{\partial x}, \qquad q_y = -k \frac{\partial T}{\partial y}, \tag{7}$$

where μ (kg m^{-1} s^{-1}) is the kinematic viscosity and k (W m^{-1} K^{-1}) refers to the thermal conductivity. This 'momentum flux' formulation determines the conserved quantities $\vec{\Phi}$ (i.e. the momentum flux $\rho\vec{v}$). The 'primitive' variables (ρ, u, v, e, p, T) can be decoded from the momentum flux variables:

$$\rho = \Phi_1, \qquad u - \frac{\Phi_2}{\Phi_1}, \qquad v = \frac{\Phi_3}{\Phi_1}, \qquad e = \frac{\Phi_4}{\Phi_1}. \tag{8}$$

 © 1997 by John Wiley & Sons, Ltd.

For an ideal gas the equations of state specify the pressure and temperature fields

$$p = (\gamma - 1)\rho(e - \tfrac{1}{2}u^2 - \tfrac{1}{2}v^2), \tag{9}$$

$$T = (e - \tfrac{1}{2}u^2 - \tfrac{1}{2}v^2)/c_v, \tag{10}$$

where γ and c_v refer to the gas constant and specific heat respectively. In this 'density-based' approach, density remains the subject of the continuity equation and the equation of state extracts the pressure field. Advantages of density-based schemes in comparison with pressure-based schemes (i.e pressure is the primary variable in the continuity equation) have been investigated by previous researchers such as MacCormack[2] and McGuirk and Page.[6] The motivation for the former approach was the explicit appearance of density in the continuity equation and the dominant role of spatial density variations in compressible flows.

DISCRETIZATION OF GOVERNING EQUATIONS

The problem domain is subdivided into linear quadrilateral elements and a local non-orthogonal (s, t) co-ordinate system is defined in each element (Figure 1(a)). The discrete conservation equations are obtained by integration of the continuum equations (1) over finite control volumes and time intervals. Each control volume is defined by further subdivision of four internal or subcontrol volumes (SCVs) within an element, each of which is associated with a control volume and its corresponding element node. The subcontrol volume boundaries or subsurfaces (SSs) are coincident with the element

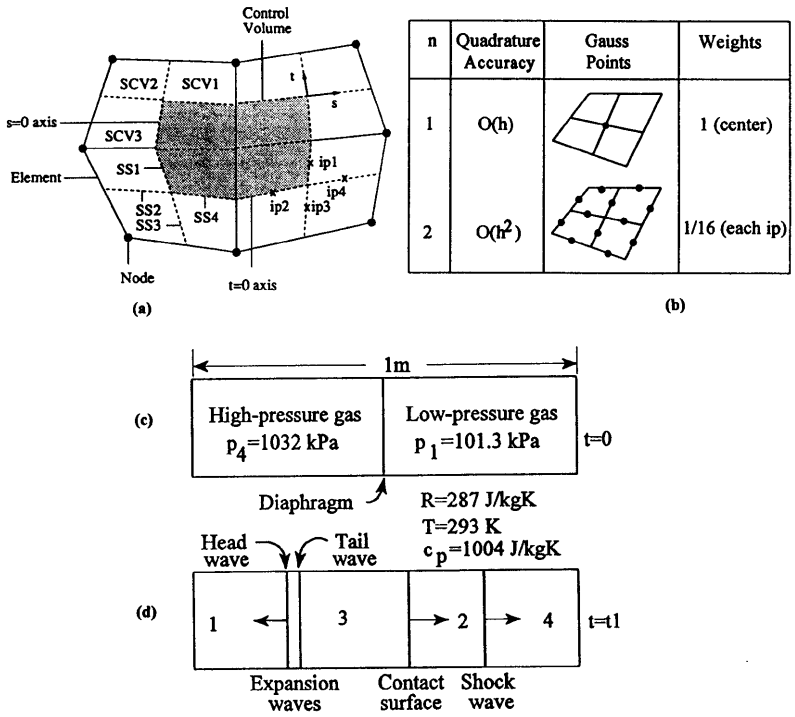

Figure 1. (a) Finite element–volume, (b) quadrature and (c), (d) shock tube schematics

© 1997 by John Wiley & Sons, Ltd.

exterior boundaries and with the local co-ordinate surfaces defined by $s = 0$ and $t = 0$. An integration point (ip) is defined as the midpoint of each subsurface.

Finite element shape functions $N(s, t)$ are used to relate global co-ordinates X_i (local node i) and scalar values Φ_i to local element values $X(s, t)$ and $\Phi(s, t)$ respectively in an isoparametric, bilinear fashion[8]

$$\Phi(s, t) = \sum_{i=1}^{4} N_i(s, t)\Phi_i, \qquad X(s, t) = \sum_{i=1}^{4} N_i(s, t)X_i, \tag{11}$$

where

$$\begin{bmatrix} N_1(s, t) \\ N_2(s, t) \\ N_3(s, t) \\ N_4(s, t) \end{bmatrix} = \frac{1}{4} \begin{bmatrix} (1 + s)(1 + t) \\ (1 - s)(1 + t) \\ (1 - s)(1 - t) \\ (1 + s)(1 - t) \end{bmatrix} \tag{12}$$

and the subscripts $i = 1, 2, 3, 4$ refer to local nodes.

For SCV1 within the shaded control volume (Figure 1(a)), equations (1) may be integrated to yield the integral conservation laws

$$\frac{\partial}{\partial t}\int_V \rho\Phi(t)\mathrm{d}V + \int_S \vec{F} \cdot \vec{\mathrm{d}n} = \int_V S_\Phi \mathrm{d}V. \tag{13}$$

The vector $\vec{F}$ consists of advection, $\vec{F}^{\mathrm{a}}$, and diffusion, $\vec{F}^{\mathrm{d}}$, parts for each conserved quantity Φ and S_Φ represents the source vector. Integration over the time interval $\Delta t = t^{n+1} - t_n$ yields the equations

$$\left(\frac{\rho J_1}{\Delta t}\right)\bar{\Phi}^{n+1} = \left(\frac{\rho J_1}{\Delta t}\right)\bar{\Phi}^{n} + \sum_{i=1}^{4} \int_{S_i} \vec{F} \cdot \vec{\mathrm{d}n} + \bar{S}_\Phi, \tag{14}$$

where J_1 is the SCV1 area. The control volume (node n) equation will be completed when each element SCV contribution is assembled into the global equations. In the present numerical scheme the advection terms are approximated with an integration point model[8] and bilinear shape function interpolation is employed for the pressure and diffusion terms. The first two transient terms in (14) require consideration of the quadrature for the spatial averages.

TRANSIENT TERM QUADRATURE

Many classical interpolation quadrature formulae evaluate the definite integral $\int_V \rho\Phi(t)\mathrm{d}V$ by a finite sum $\sum_{i=1}^{n} \rho w_{ni}(\Phi(\vec{x}_{ni}))$, where w_{ni} are weight factors and $\vec{x}_{ni}$ are quadrature points (or Gauss points). If the Gaussian quadrature is exact for orthogonal polynomials with degree n (i.e. $1, x, x^2, \ldots, x^n$), then its order of accuracy is $\mathcal{O}(h^{2n})$, where h represents an element length. For example, exact integration of a constant requires an $\mathcal{O}(h)$ rule (i.e. one Gauss point at a node) and exact integration of a line requires an $\mathcal{O}(h^2)$ rule (i.e. two Gauss points or one Gauss point along each element subsurface). The weights and their locations for first-order and second-order quadratures for the finite volume–element geometry are illustrated in Figure 1(b).

The selection of a quadrature rule involves the question of cost and accuracy. If the quadrature accuracy is too low (i.e. first-order), then the quadrature error will exceed the discretization error (i.e. second-order convection model) and adversely affect the solution accuracy. If the quadrature order is too high (i.e. third-order), then the quadrature error is much less than the discretization error and the additional computational effort would be wasted, because the overall accuracy would be limited by

 © 1997 by John Wiley & Sons, Ltd.

the discretization error. The effect of both first-order and second-order models on compressible flow simulations will be examined through the following shock tube problem.

SHOCK TUBE PROBLEM

The shock tube problem consists of a constant area duct with a length $L = 1$ m and a diaphragm at $x = 0{\cdot}5$ m which initially divides the tube into a low-pressure region, $P_1 = 101{\cdot}3$ kPa, and a high-pressure region, $P_2 = 1032$ kPa (Figure 1(c)). After the sudden removal of the diaphragm a contact surface (temperature field discontinuity) and normal shock wave propagate into the low-pressure region and rarefaction waves propagate in the opposite direction (Figure 1(d)). In the numerical simulations a direct banded algebraic solver with single-precision accuracy on a Sun 486 Sparcstation was employed.

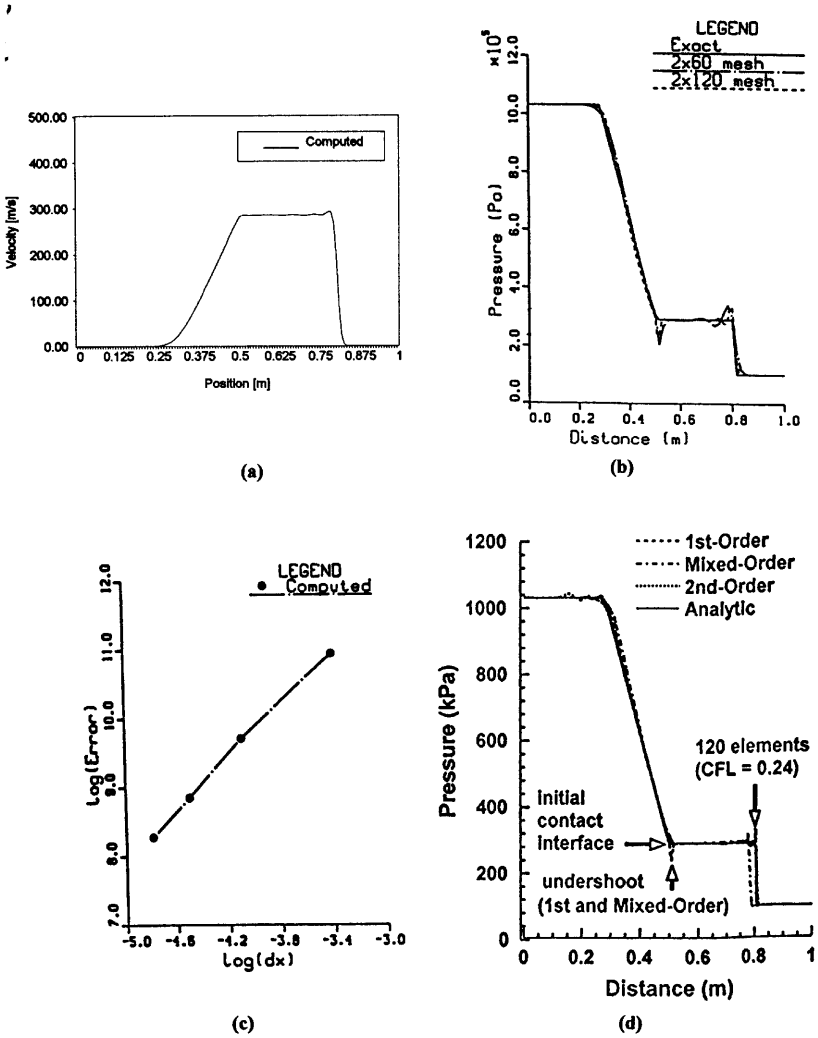

Figure 2. Shock tube problem ($t = 0{\cdot}56$ ms): (a) velocity, (b) pressure, (c) grid refinement and (d) volumetric quadrature results

© 1997 by John Wiley & Sons, Ltd.

The results from transient simulations to $t = 0{\cdot}56$ ms with a first-order quadrature are illustrated in Figures 2(a) (velocity) and 2(b) (pressure). In each simulation (Figure 2(b)), pressure oscillations appear in the vicinity of the initial contact discontinuity and the shock wave. Since the shock wave and expansion waves move at supersonic and subsonic speeds respectively, a first-order quadrature which approximates volume averages at one node may lack the correct upstream and downstream influences in transonic regions (i.e. initial contact discontinuity region). In other words, a first-order approximation in a control volume near the initial discontinuity will overestimate the local velocity (i.e. lack of upstream subsonic influences) and hence underestimate the gas pressure (Figure 2(b)).

It is anticipated that this anomaly will diminish as grid refinement is effected. Figure 2(c) illustrates the reduction of pressure solution error (i.e. average pressure level between diaphragm and shock locations minus exact result) with grid refinements (2×30, 2×60, 2×120 and 2×240 grids). Figure 2(c) shows that the approximate quadratic reduction of solution error (i.e. nearly 2:1 slope) with grid size suggests a second-order formulation accuracy.

Figure 2(d) illustrates the effects of quadrature error on the contact surface resolution and the shock speed. Both first-order and mixed-order (i.e. first-order at time level $n+1$ and second-order at time level n) schemes yield pressure oscillations near the initial contact interface (Figure 2(d)). However, a second-order model with an identical grid resolution (2×120 elements) and Courant–Friedrich–Lewy number ($CFL = 0{\cdot}24$) captures this interface without oscillatory deviations from the exact results (Figure 2(d)). Therefore the results indicate that the second-order quadrature improves the adverse effects of slow shock wave speed and pressure undershoots associated with first-order approximations.

The important of proper upstream and downstream influences in the accuracy of subgrid convection models is well known in the literature. The present work indicates that these influences can also play an important role in transient term approximations. A first-order volumetric quadrature represents the central node influence. However, a second-order quadrature with a conventional backward difference includes upstream and downstream integration point influences as well as central node influences and therefore permits more accurate predictions of shock wave speed and pressure profiles in transonic regions.

CONCLUSIONS

A finite element formulation of the Navier–Stokes equations for compressible flows has been applied to the transient shock tube problem. First- and mixed-order quadratures produce solution anomalies in regions with a transonic character as well as inaccurate predictions of the shock wave propagation. However, the results indicate that the inclusion of a second-order transient model improves the shock and rarefaction wave resolution and positioning because of the correct upstream and downstream influences in the numerical quadrature.

ACKNOWLEDGEMENTS

The author would like to thank Dr. G. E. Schneider at the University of Waterloo for his assistance with this work. Also, the valuable suggestions from the manuscript review process are gratefully acknowledged.

APPENDIX: NOMENCLATURE

c	speed of sound (m s^{-1})
CFL	Courant–Friedrichs–Lewy number, $c\Delta t/\Delta x$
t	time (s)

 © 1997 by John Wiley & Sons, Ltd.

x, y Cartesian co-ordinates

Greek letters

ϕ integration point field variable
Φ nodal field variable

Subscripts

i integration point
n degree of accuracy

Superscripts

n previous time level
$n+1$ current time level

REFERENCES

1. L. Crocco, 'A suggestion for the numerical solution of the steady Navier–Stokes equations', *AIAA J.*, **3**, 1824–1832 (1965).
2. R. W. MacCormack, 'A numerical method for solving the equations of compressible viscous flow', *AIAA Paper 81–0110*, 1981.
3. D. Pepper and J. Humphrey, 'A hybrid finite element method for compressible flow', *AIAA Paper 90–0399*, 1990.
4. R. Lohner, K. Morgan and O. C. Zienkiewicz, 'The solution of the non-linear hyperbolic equation systems by the finite element method', *Int. j. numer. methods fluids*, **4**, 1043–1063 (1984).
5. K. C. Karki and S. V. Patankar, 'Pressure based calculation procedure for viscous flows at all speeds in arbitrary configurations', *AIAA J.*, **27**, 1167–1174 (1989).
6. J. J. McGuirk and G. J. Page, 'Shock capturing using a pressure-correction method', *AIAA J.*, **28**, 1751–1757 (1990).
7. M. Zlamal, 'Curved elements in the finite element method', *SIAM J. Numer. Anal.*, **11**, 347 (1974).
8. W. J. Minkowycz, E. M. Sparrow, G. E. Schneider and R. H. Pletcher, *Handbook of Numerical Heat Transfer*, Wiley, New York, 1988.
9. P. L. Roe, 'Approximate Riemann solvers, Parametric vectors and difference solutions', *J. Comput. Phys.*, **43**, 357–372 (1981).
10. J. Van Doormal, 'Numerical methods for the solution of incompressible and compressible fluid flows', *Ph.D. Thesis*, University of Waterloo, 1985.
11. G. F. Naterer and G. E. Schneider, 'Use of the second law for artificial dissipation in compressiblee flow discrete analysis', *AIAA J. Thermophys. Heat Transfer*, **8**, 500–506 (1994).

© 1997 by John Wiley & Sons, Ltd.